ARMA 19–484

Stability Analysis of an Underground Limestone Mine Using Terrestrial Laser Scanning with Stochastic Discrete Element Modeling

Monsalve, J.J., Baggett, J.G., Soni, A. and Ripepi, N.

Mining and Minerals Engineering Department, Virginia Polytechnic Institute & State University, Blacksburg, Virginia, United States

Hazzard, J.

ITASCA Consulting Group, Minneapolis, Minnesota, United States

ABSTRACT: The underground limestone mining industry has one of the highest fatality rates compared to all other types of mining in the United States (MSHA, 2016). Ground control issues heavily contribute to these fatalities. According to the National Institute for Occupational Safety and Health (NIOSH, 2011), structurally controlled instability is a predominant failure mechanism in underground limestone mines. Existing analysis methods, such as the limit equilibrium method, do not represent the real structure and behavior of a rock mass in-situ. The Discrete Element Method (DEM) when coupled with representative Discrete Fracture Networks (DFN) has been proven to provide accurate models of the actual response of a rock mass undergoing excavation. However, considering the statistical nature of DFN's, multiple simulations need to be run in order to obtain statistically significant results of the model. The following paper introduces a stochastic approach for analyzing rock block falls in underground excavations. This approach utilizes DEM (Itasca's 3DEC) and DFN's representing virtually mapped discontinuities obtained from terrestrial laser scans. The numerical models were carried out considering rigid blocks. Failed blocks were defined as those blocks that had displaced more than 2 cm and presented velocities indicating that the block was still in movement. This approach allows engineers to define the probability of block failure based on the geometry and weight of failed blocks formed by the intersection of discontinuities in the section of interest, as well as to define kinematics of the blocks. Such information can provide mining operators control measures to evaluate, map and mitigate risks associated with rock falls in underground mines, ultimately improving safety in the underground limestone industry.

1. INTRODUCTION

Ground control instability issues are one of the main causes of accidents and fatalities in underground mining in the U.S. (MSHA, 2016). Within these ground control issues, structurally controlled instability is one of the main failure mechanisms in underground limestone mines (NIOSH, 2011). This type of instability takes place when two or more structural sets intersect forming rock blocks that can fall as the excavation advances (Goodman & Shi, 1985) (Hudson & Harrison, 2000). Additionally, in room and pillar mining operations, a rock fall due to structurally controlled instability may affect the shape of a pillar, subsequently reducing its strength parameters, and ultimately leading to a pillar failure (Brady & Brown, 1985). This failure mechanism depends on several factors, such as the structural condition of the rock mass (including number of discontinuity sets, orientation, spacing and size of discontinuities), the mechanical properties of the discontinuities, and the orientation and size of the excavations. These structural features are generated as a response to the stress changes throughout the geological history of the rock mass, and they can vary from location to location and even within the same mine. In order to evaluate the block fall risk these discontinuities should be adequately identified, measured and mapped.

Previous research has shown that terrestrial laser scanning (TLS) and photogrammetry technologies are able to obtain adequate density point clouds for virtual discontinuity mapping (Lato, Diederichs, Hutchinson, & Harrap, 2009) (Cacciari & Futai, 2017) (Monsalve J. , Baggett, Bishop, & Ripepi, 2019). The information obtained from these mapping processes can be used to perform engineering analyses aimed at identifying the potential blocks that form in the excavation. In an earlier work, Monsalve, et al. (2018) describe and compare the two current analysis methodologies to evaluate structurally controlled instability: the Limit Equilibrium Method (LEM) and the Discrete Element Method (DEM). The authors concluded that the DEM with detailed structural information, such as the one obtained from TLS by virtual discontinuity mapping and Discrete Fracture Network (DFN) generation, provides both deterministic and stochastic results to better understand the rock mass

behavior under excavation (Monsalve J. , Baggett, Bishop, & Ripepi, 2018).

The DEM is a numerical analysis tool that can simulate the behavior of a discrete body, such as a rock mass, under either static or dynamic loads. The blocks that constitute the rock mass are formed by intersecting explicit fractures whose locations, orientations and dimensions are necessary to define the model (Jing & Stephansson, 2007). Specifically, 3DEC has the capability to generate Discrete Fracture Networks (DFNs) and use them to cut through a block until a structural condition similar to that of the rock mass is reproduced (ITASCA, 2016). Each DFN is composed by a number disk shaped fractures. When a block is cut with a DFN, each fracture belonging the DFN must completely bisect a block. If a fracture is in between two different blocks, both blocks will be completely bisected, even if this fracture is smaller than these blocks. Due to this, in a final fracture model it is not possible to have isolated circular fractures as the ones belonging to the DFN. Figure 1 shows a comparison between the DFNs and the final fractured model. It is observable that even though there are similar patterns between both, they are not identical. Due to this discrepancy, it is important to calibrate this model so the final structural conditions are as closely representative of those observed in the field and mapped from the laser scans.

DFNs are a geometrical representation of the structures mapped from the rock mass, based on statistical information of their orientation, size and frequency (Pierce, 2017). Their nature is merely statistical. If further stability analyses are intended, these require a stochastic modelling approach (Monsalve J. , Baggett, Bishop, & Ripepi, 2019). Different authors have performed stochastic stability analyses of failure in fractured rock masses using DFNs; however, they have used LEM analysis. Grenon & Hadjigeorgiou (2003) evaluated the stability of wedges in underground mines at the periphery of mining stopes by integrating a 3D joint network generation model with a 3D limit equilibrium software package. Fu & Ma (2012) presented an algorithm that evaluates progressive failure in rock masses based on the LEM and the key block theory. This method would be extended later to perform a stochastic analysis of progressive failure in rock slopes and underground excavation, obtaining probability density functions indicating the amount of failed blocks (key blocks) and their volumes (Fu, Ma, Qu, & Huang, 2016). Grenon, Landry, Hadjigeorgiou, & Lajoie (2017) compared different fracture network models and evaluated the stability of a drift in an underground mine with stochastic limit equilibrium anlysis based on previous work. Similarily, Rogers, Bewick, Brzovic, & Gaudreau (2017) performed stochastic LEM analysis in an underground excavation, obtaining the DFN's information from photogrammetric surveys. As is shown by these limited number of studies, there is a lack of research in stochastic methods using the DEM.

The following paper presents the stability analysis of a previously defined case study mine based on a stochastic discrete element model approach. This analysis method is performed by running multiple iterations of a discrete element model in 3DEC that simulates a 20-meter long section of the excavation. This method resulted in an estimate of probability for the number of failed blocks and the volume of the unstable mass of rock.

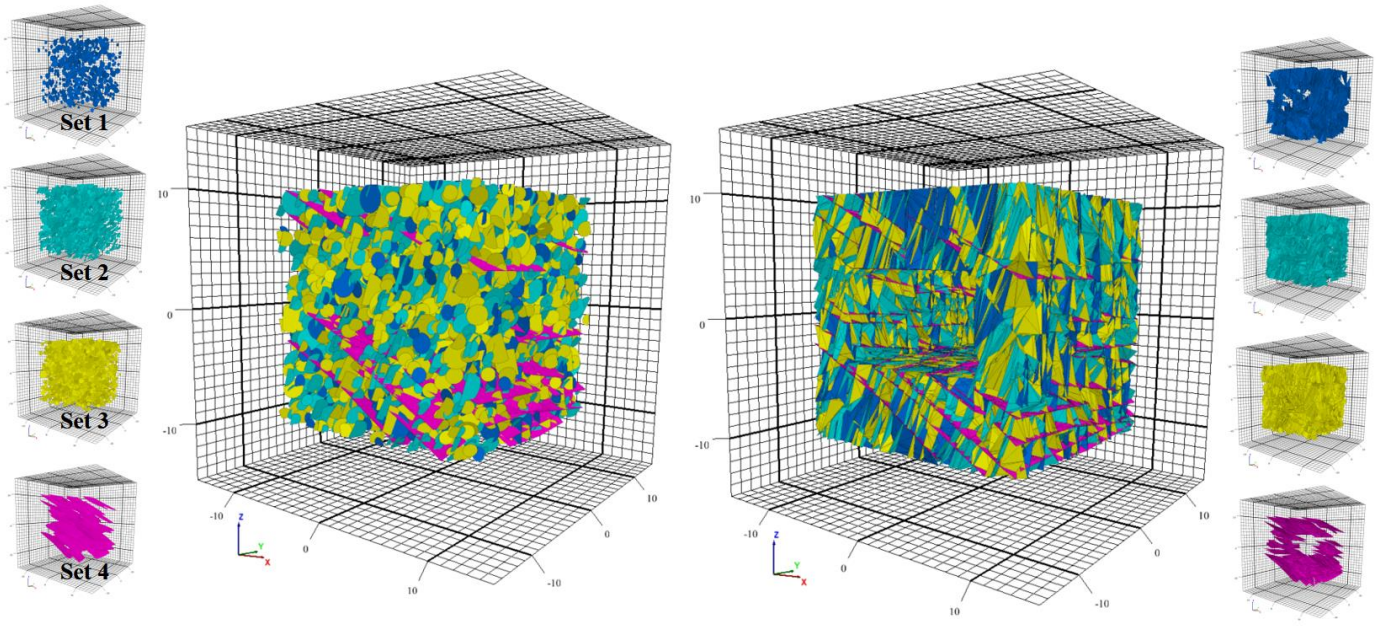

Figure 1. Comparison between DFNs and actual fractures in the model.

2. GEOTECHNICAL CONDITIONS

In previous work, Monsalve et al. described the geotechnical conditions of the CSM. This operation extracts a 30 m thick and 30° dipping limestone body with a room and pillar mining method with eventual stopping. The stopes are conformed along the strike of the body, when the seam is consistent and thick enough. These are conformed by top and bottom drifts, 12.8 m wide and 7.6 m high, which are separated by a 15 m sill which is extracted by vertical long hole drilling (Sill and pillar mining). The stopes are supported by 24 m by 24 m pillars. This rock has a UCS of 159.2 MPa ± 21.25 MPa, a tensile strength of 6.3 MPa ± 1.99 MPa and a Young's modulus of 64.11 GPa ± 2.37 MPa. In addition to this, an average GSI value of 75 was reported throughout the area of interest. The deepest point in the mine is approximately 700 m below ground surface and is exposed to a maximum vertical stress close to 20 MPa.

As described in the above mentioned previous work, according to the risk/Hazard Assessment Chart proposed by Martin, Kaiser, & Christiansson (2003), the main cause of instability in this excavation is due to gravity-induced structurally controlled block movement, which agrees with the observed failure conditions in the mine (Monsalve J. , Baggett, Bishop, & Ripepi, 2018). If the horizontal stress is assumed to be the principal maximum stress and 1.2 times higher than the vertical stress, for the mine to be under stress induced failure the excavations should be deeper than 750 m, as it is presented in Figure 2. Considering that the deepest level in the mine is 700 m below ground surface, stress induced failure mechanisms are unlikely to be encountered in this mine.

The ore body is located in the limb of a regional syncline structure. From terrestrial laser scanning and virtual discontinuity mapping, the authors were able to identify four main discontinuity sets. These discontinuity sets were classified as: Set 4, which corresponds to the bedding planes and contacts between rock units, which are almost parallel to the tunnel orientation and has a mean dip of 29°; Set 1, which is almost perpendicular to the tunnel orientation and presents a sub-vertical dip; and Sets 2 and 3, which are oblique joints with a steep dip. These four identified structural sets agree with the model of joints in folded sediments proposed by some authors, where Set 1 corresponds to Dip joints, Set 2 and 3 could be classified as oblique or shear joints, and Set 4 corresponds to bedding planes, as can be observed in Figure 3 (Brady & Brown, 1985) (Blyth & de Freitas, 1984).

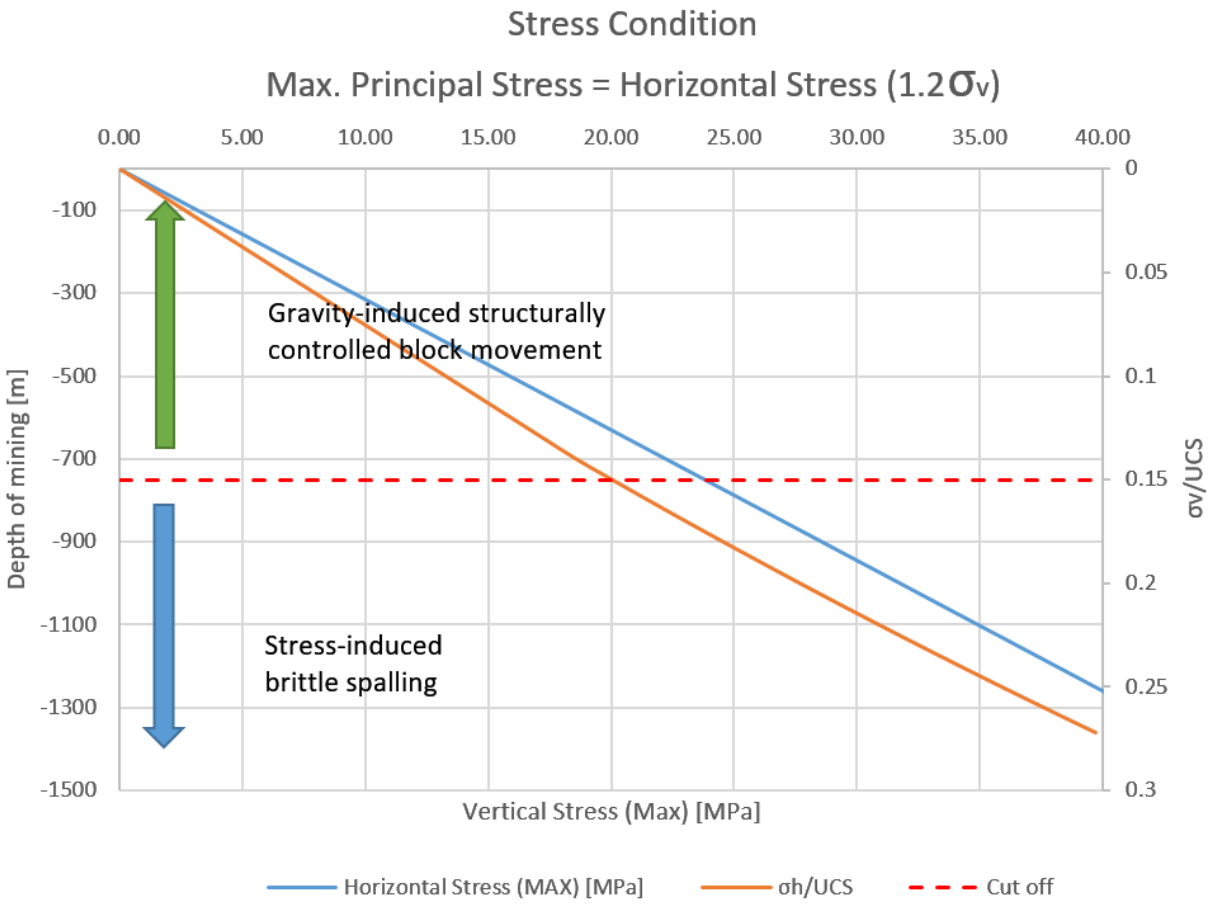

Figure 2. Failure mechanisms depending on the depth of the mine based on the risk/Hazzard Assessment chart proposed by Martin, Kaiser, & Christiansson.

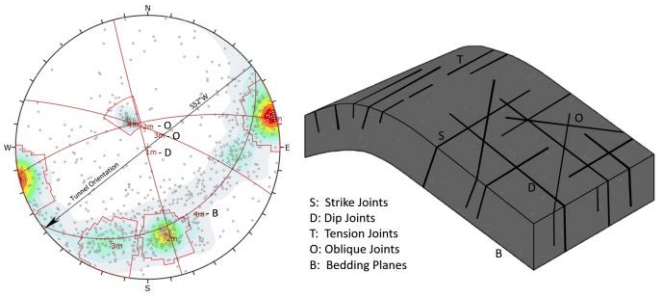

Figure 3. Relation between structural sets defined in the CSM and Jointing model in folded sediments.

In addition to this, additional field work aimed at measuring the mechanical properties of the discontinuities was carried out. In general, it was determined that all discontinuity sets are mainly very closed. The weathering conditions ranged between decolored and fresh for all the discontinuity sets. The majority of the discontinuities were completely damp, except for some discontinuities located closer to karst features, which were encountered wet and a few of them were dripping. Fifty-four percent of the mapped discontinuities did not present any filling material, while 22% were filled with calcite and the other 24% were filled with mud, mainly coming from the karsts. In addition, 64 % of the fractures from all the families presented a joint roughness coefficient (JRC) between 2 and 4, while the other 38 % of the fractures presented higher JRCs between 6 and 10. The bedding planes were the fractures that presented the highest JRCs. In addition to this, tilt tests were performed which obtained friction angle values ranging from 30° to 35°.

3. ANALYSIS METHODOLOGY

Initially, preliminary models were developed considering simple tunnel geometries and simplified DFNs. These initial models were calibrated and improved until the model closely represented the rock mass structure and the excavation section. The final model represents a 20-m long section of the excavation and takes into account the four mapped discontinuity sets. The model was run for 40000 cycles after excavation, with a time step of 3.81x10-6 seconds, taking 6 hours of processing time. The hardware consisted of a MSI laptop computer with 16 Gb of RAM and a 7th generation Core i7 processor. Once the model was run, a function was written to mark failed blocks (Fekete & Diedrichs, 2013). The failed blocks were defined as those blocks that had displaced more than 2 cm and presented velocities higher than 5x10-5 mm/s indicating that the blocks were in movement (Curden & Varnes, 1996). Then information about the blocks was stored in a text file. This information included block number, block volume, block mass and velocity.

As mentioned earlier, due to the stochastic nature of the DFNs, the results obtained just from one simulation are not representative of the overall response of the rock mass under excavation. Due to this, the model was run 30 times, reporting the same information for each iteration. This was done by generating a master file which ran the model several times and varying the random seed number to ensure every result was different. The iteration number was stored in the text file along with the block information. This enabled the performance of further analyses on the extracted information. In order to validate the models, the results were compared with the 3 dimensional point clouds obtained from the laser scans. Two dimensional sections from both models were extracted and compared.

The text file was imported into an excel file where information was processed and analyzed. The parameters that were evaluated were total number of failed blocks and total volume of failed blocks. These two parameters give insight into the amount of rock fall that can occur in the excavation given certain structural condition in the rock mass. The statistical analysis software JMP was used to perform a statistical analysis on the results (Proust, 2018). Probability Density Functions were fitted and validated for these two parameters, allowing the probability of block failure in the 20 m long section to be estimated. On the other hand, the x, y and z velocity components were converted to stereographical data. This information allowed the kinematics of the failed blocks to be better interpreted.

4. 3DEC MODEL

This section explains how the 3DEC model was programmed and describes the conditions and assumptions considered in this study.

Initially, a DFN was generated for each discontinuity set present in the rock mass. These DFNs were defined within a control volume of 20 m x 20 m x 20 m. The input parameters considered for this were obtained from the authors' (Monsalve J. , Baggett, Bishop, & Ripepi, 2019) previous research . The parameters required to generate the DFNs were orientation, size and density. For orientation, a Fisher distribution was considered for all the discontinuity sets. Dip, dip direction and K values are presented for all discontinuity sets in Table 1. In order to simplify the model, the y axis was defined parallel to the tunnel orientation (N52°E). Due to this, all discontinuity sets were rotated 52° counterclockwise to maintain their orientations respective to the excavation. For Sets 1, 2 and 3, a log-normal distribution for the size was considered based on the values obtained from the laser scans. A function was written to consider log-normal distributions for joint size, since the 3DEC DFN generator does not

include these distributions for this parameter. The values measured from the laser scans were not considered for Set 4, since it corresponds to the bedding, which extends consistently along the rock mass. Instead of this, a Gaussian distribution, with a mean of 9 m and a standard deviation of 1 m, was used to generate this DFN, allowing it to better represent this family. The area of fractures per unit volume (P32) was considered as the density parameter. The P32 value was calibrated until the measured number of fractures per unit length of scan line (P10) in the resulting fracture model reached values close to those obtained from the virtual discontinuity mapping.

The geometry of the excavation was based on the general mine design. The section is rectangular with a width of 12.8 m and a height of 7.6 m. This geometry was modeled in Rhinoceros and imported into 3DEC using Griddle (ITASCA, 2017). Two sections in the geometry were considered: 1) an inner section, considered as the fractured rock mass which contained the excavation; and 2) an external section, considered as the massive rock mass for the sake of the simplicity for the model. After the geometry was imported, the blocks were cut with the DFNs. The cutting order was a relevant parameter to simulate the rock mass structure, since it altered significantly the fracturing model. For this study, the set bedding planes were used to cut the model first, followed by Set 1 which corresponded to dip joints, followed by Sets 2 and 3 which corresponded to shear joints. Figure 4.a. shows the jointing model after the DFNs cut the initial block. Figure 4.b) illustrates the inner section, representing the fractured rock mass with the excavation. In addition to this, Figure 4.c) displays a two dimensional section of the excavation, where the fractures can be noticed.

Table 1. Statistical Summary of the joint properties for each joint set.

SET / PARAMETERS		S1 N=157	S2 N=127	S3 N=97	S4 (Bedding) N=45
Orientation	Dip [°]	88	68	75	29
	Dip Direction [°]	255	348	21	144
	K (Fisher)	103.9	102.4	69.5	197.3
Size	Distribution	Log-normal	Log-normal	Log-normal	Normal
	Mean	0.353	0.318	0.018	9
	Standard deviation	0.659	0.772	0.749	1
Density	Input area of fractures per unit volume (P_{32})	0.1	0.4	0.4	0.5

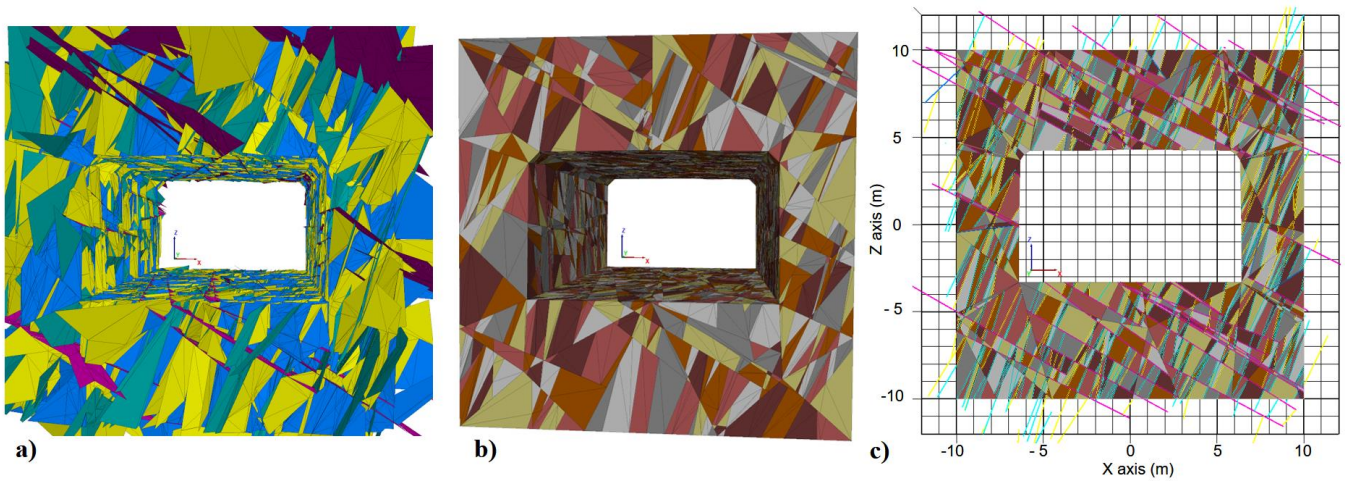

Figure 4. a) Jointed model b) Inner Section of the Geometry indicating the Jointed rock mass. c) XZ 2-Dimensional displaying the excavation the rock blocks and joints.

Considering that the main failure mechanism defined was gravity-induced, structurally controlled block movement, and that there was no evidence of failure resulting from high stresses, it was decided to use rigid blocks in the model. This means that the only deformation observed in the simulation occurs along discontinuity planes and the blocks do not change their geometries. The gravity was set as 9.81 m/s2. Additionally, the external section of the geometry was fixed, preventing it from displacing. Thus, the only blocks that were displaced were the ones belonging to the fractured rock mass section.

The intact rock properties were obtained from previous laboratory testing performed by the mine operator. Blocks were assigned a density of 2700 kg/m3 and were assumed to be infinitely stiff (rigid). Furthermore, discontinuity properties were assumed to have a friction angle of 30° and no cohesion based on tilt tests and field observations. These values represented the worst discontinuity strength conditions. A joint shear stiffness of 30 MPa/mm and a joint normal stiffness of 300 MPa/mm were used. These values were obtained based on the work performed by Bandis, Lumsden, & Barton (1983).

Once the model was set up, it was cycled 500 times to reach initial equilibrium before excavation. After these initial cycles were run, the material inside the tunnel was excavated and run for an additional 40000 cycles. Once, these cycles were finished, the failed blocks analysis stage proceeded.

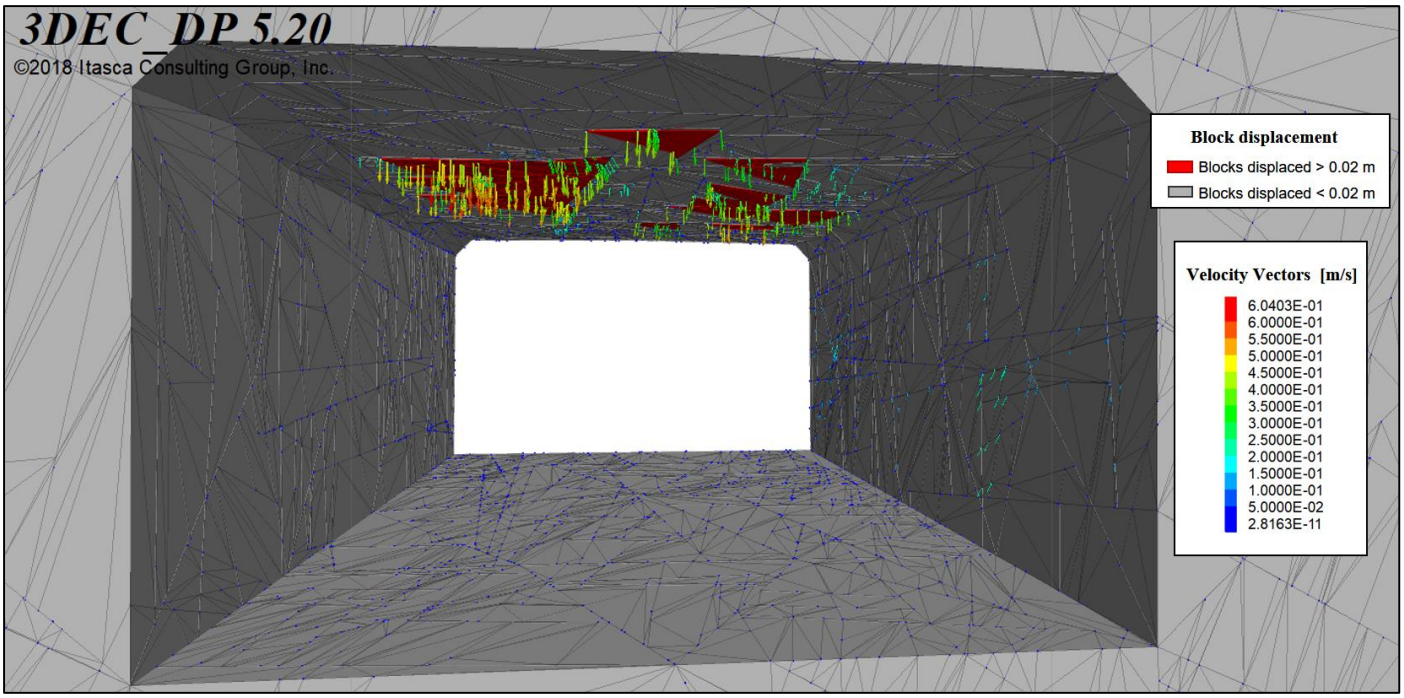

Figure 5. Discrete element model of the study area indicating failed blocks.

5. RESULTS AND DISCUSSION

Figure 5 shows the results obtained from one of the simulations in 3DEC. In the model, red indicates blocks that defined as failed blocks, while grey indicates those blocks that have not yet failed. Velocity vectors also are marked, indicating blocks that are still displacing. In this particular simulation the maximum displacements obtained are 4.62 cm and the maximum block velocities obtained are 0.6 m/s. Additionally, the figure shows that the majority of failed blocks on the roof presented geometries ranging from oblique triangular pyramids to irregular prisms, which are shown isolated in Figure 6. Not only did working with rigid blocks showed an acceptable rock mass behavior, but this assumption significantly reduced the processing time as well.

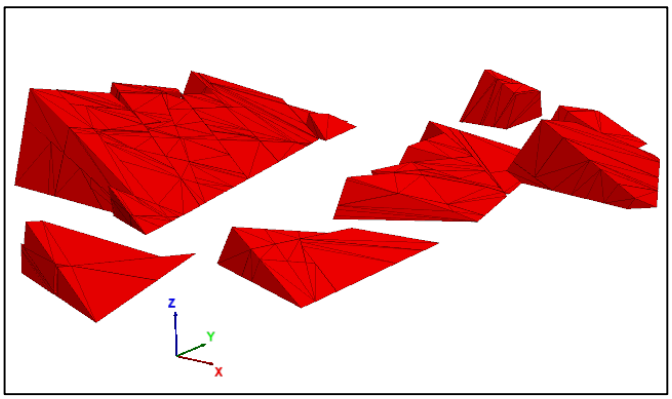

Figure 6. Typical geometries of failed blocks in the discrete element model.

Results obtained from the simulations were compared with previously Laser-scanned sections. Taking into account that the 3DEC models were stochastic, they were not meant to match exactly the laser scanned sections. However, the blocks formed in the numerical model still shared similar volumes and shapes to those observed in the laser-scanned sections. Figure 7 compares two 2-dimensional sections, one extracted from laser scans and the other extracted from numerical models. Results from both show similarities between the locations, sizes and shapes of the blocks. Figure 8 shows a failed block from 3DEC matching the gap left from a failed block in a laser scanned section in the study area. These results indicate that the structural model obtained from the virtual discontinuity mapping somehow adequately represents the structure of the rock mass.

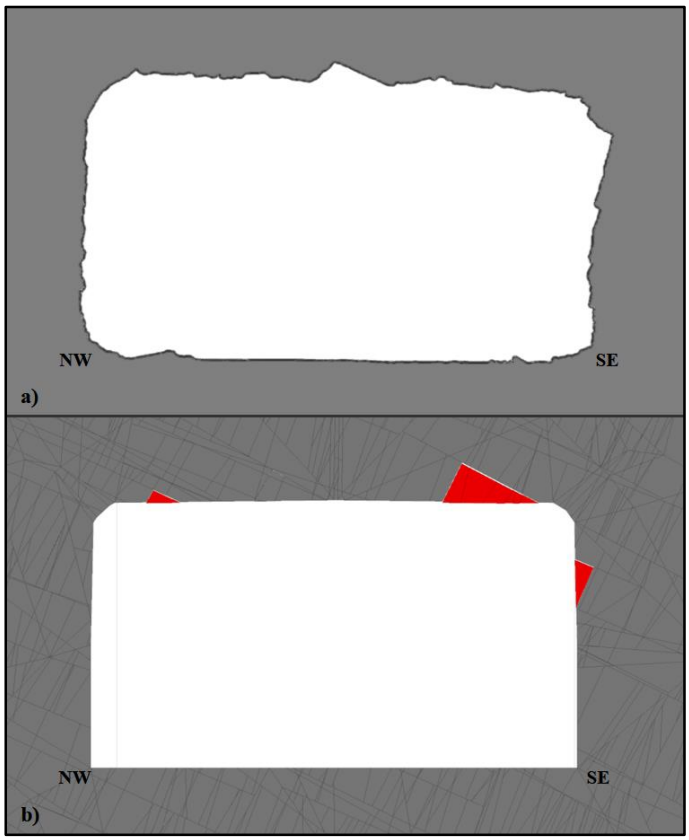

Figure 7. Comparison between 2 dimensional section obtained from a) Laser Scanning Point clouds and b) Discrete Element Model.

The stochastic modelling stage resulted in 30 discrete element models and took around 180 hours. Figure 9 shows some of the models obtained from this analysis. As mentioned earlier, information for each of the 3,146 failed blocks was recorded. Two main parameters were evaluated from the models: the number of failed blocks per iteration, and the total volume of failed blocks per iteration. This information was analyzed in the statistical software JMP, where probability density functions were defined for these parameters. The volume of failed blocks was fitted to a log-normal distribution, with a mean of 2.60 m3 and a standard deviation of 0.49 m3. This distribution was validated with the Kolmogorov's D goodness of fit test. On the other hand, the number of failed blocks was distributed normally with a mean value of 104.86 and a standard deviation of 47.58. Similarly, this distribution was validated using the Shapiro-Wilk W goodness of fit test. These results indicate that considering the present structural condition in this section of the mine, there is 35% probability for a total volume of 10 m3 of rock blocks to fall in 20 m of tunneling advance. Results obtained from this methodology offer engineers an accurate tool to estimate the mass of failed blocks in excavations under structurally controlled failure mechanism.

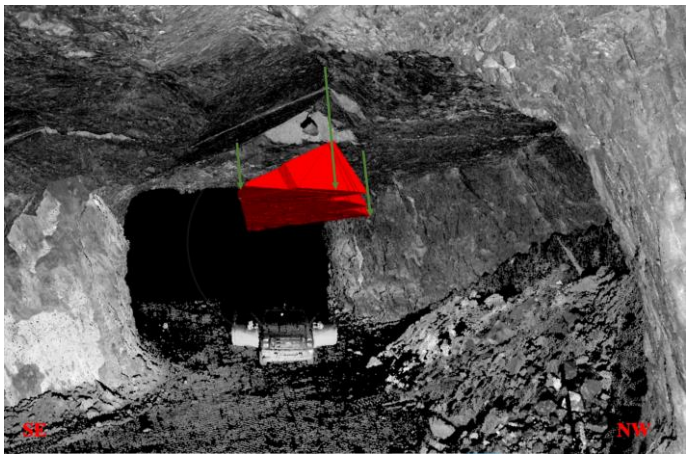

Figure 8. 3DEC failed block matching a gap left from a failed block in a laser scanned section.

Once the failed blocks probability was estimated, as described in previous section, a block kinematics analysis was performed. The velocity vectors from all the models were transformed into spherical coordinates, allowing them to be presented in a stereonet. Figure 10 shows a model of failed blocks in the roof and in the south-east wall of the excavation, as well as the velocity vectors for all failed blocks. The figure demonstrates that the majority of the blocks were falling vertically from the roof; however, other vectors were concentrated more towards the NW. These vectors represent blocks falling from the south-east wall towards the excavation.

Results obtained from this stochastic model can be extended to any sector of the mine sharing similar structural condition as that mapped on the study area. If a different structural condition is reported, these models must be repeated considering the new structural setting. The methodology described in this work can be applied in any underground limestone mine presenting a structurally controlled failure mechanism, and the results obtained from these analyses can be used to define probability of block failure. Similarly, the data and information resulting from this work can be integrated into a risk management system to control risks associated with rock fall in a mine, ultimately improving safety in the operation.

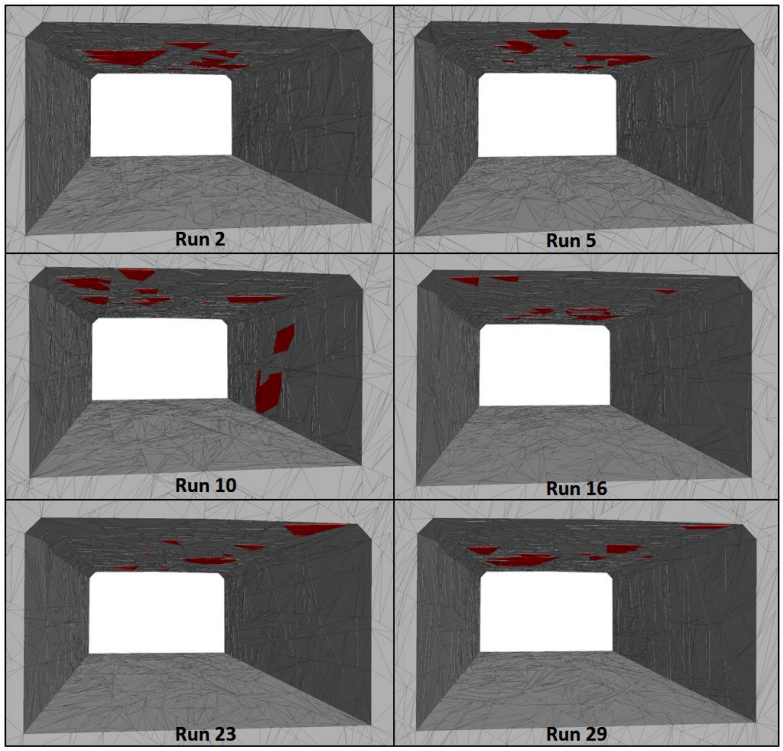

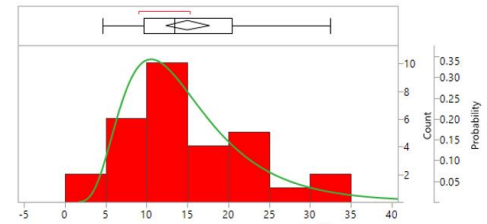

Total volume of failed blocks [m³]

Summary Statistics	
Distribution	Log-Normal
Mean	2.60
Standard Deviation	0.49

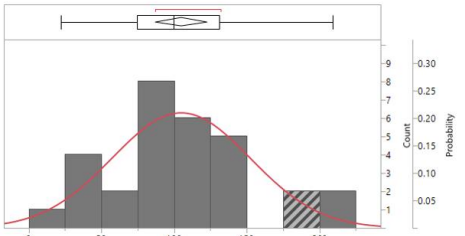

Number of failed blocks [m³]

Summary Statistics	
Distribution	Normal
Mean	104.87
Standard Deviation	47.58

Figure 9. Stochastic approach to block failure analysis.

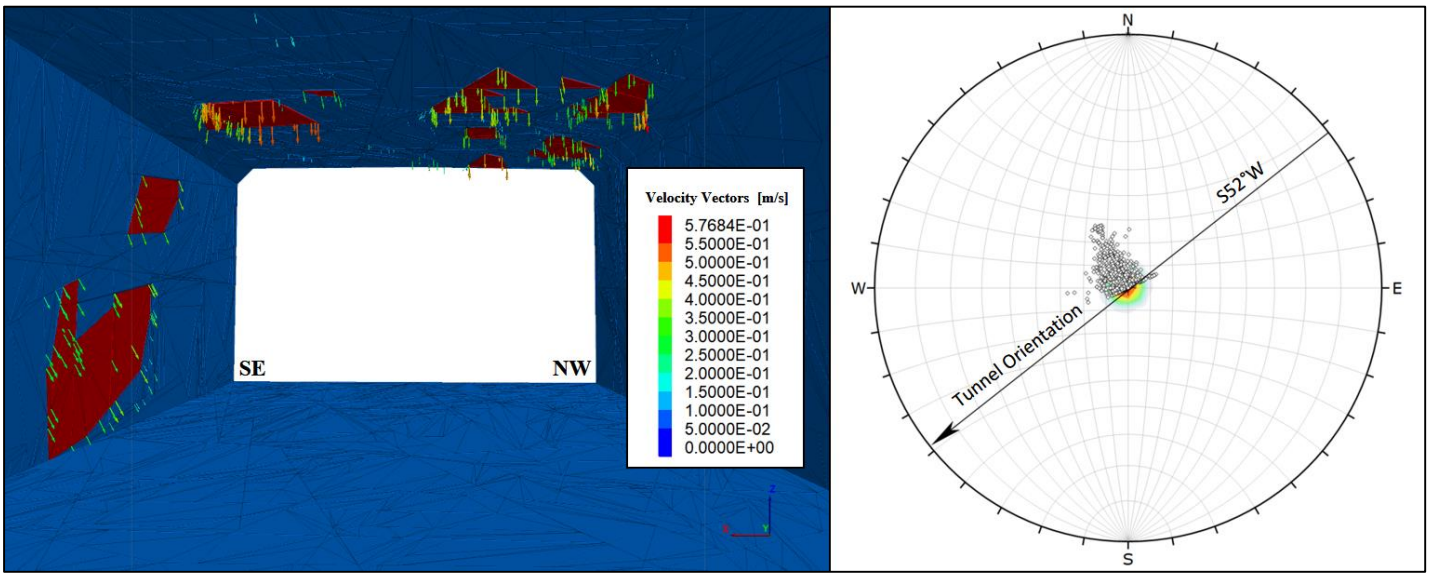

Figure 10. Stereographical analysis of block kinematics.

6. FURTHER WORK

Based on the results of this work, a number of different research opportunities are identified. This methodology can be extended to rock support design under structurally controlled instability. Pillar strength on fractured pillars could also be analyzed by using stochastic discrete element modelling with 3DEC. In underground mines where stresses can be an additional issue, this methodology may also be applied if deformable blocks are considered, even though, the analysis time may significantly increase.

7. CONCLUSIONS

This work presented a methodology for analyzing the stability of an underground limestone mine under structurally controlled failure. This methodology integrated results from terrestrial laser scanning with Discrete Fracture Networks and Discrete Element

Modelling software. The following conclusions can be drawn from this work:

1. Terrestrial laser scanning was successfully integrated with Discrete Element Modelling by applying discrete fracture networks in the model. The information obtained from virtual discontinuity mapping in the laser scans was used as inputs for generating the DFNs which were then used to build the 3DEC model.

2. It is important to have a general understanding of the geological model of the rock mass. This knowledge dictates how the 3DEC model is built. In this work, the joint set corresponding to the bedding planes was used to first cut the blocks than the other sets. This enhanced the results of the rock mass model.

3. In this study, working with rigid blocks was an acceptable assumption, which yielded results similar to those observed in the field. Should this methodology be used in an underground excavation presenting both structurally controlled and stress controlled failure mechanisms, it is recommended to work with deformable blocks, which may increase significantly the processing time.

4. The results obtained from the model agreed with the failure mechanisms observed in the field. The results were also comparable with those obtained from laser scans, indicating that the parameters considered in the model were acceptable.

5. Considering the stochastic nature of DFNs, it is necessary to extend the discrete element models to a stochastic approach in order to obtain significant results. A stochastic modelling approach allows engineers to measure the probability of block failure in a section of the excavation. This methodology could also be extended to rock support design and pillar strength determination.

6. The present methodology can be used as a method for rock fall hazard identification in underground limestone mines. It can be easily integrated into a risk management system, allowing engineers and mining operators to have greater control over possible block failures, to reduce ground control related accidents, and to improve the safety of these operations.

8. ACKNOWLEDGMENTS

This work is funded by the NIOSH Mining Program under Contract No. 200-2016-91300. The authors would like to thank ITASCA for their support and guidance during this project. Views expressed here are those of the authors and do not necessarily represent those of any funding source.

9. REFERENCES

Bandis, S., Lumsden, A., & Barton, N. (1983). Fundamentals of rock Joint Deformation. International Journal of Rock Mechanics, Mining Sciences & Geomechanics, 249-268.

Blyth, F., & de Freitas, M. (1984). A Geology for Engineers. London: ELSEVIER.

Brady, B., & Brown, E. (1985). Rock Mechanics for Underground Mining. UK: Chapman & Hall.

Cacciari, P., & Futai, M. (2017). Modeling a Shallow Rock Tunnel Using Terrestrial Laser Scanning and Discrete Fracture Networks. Rock Mechanics and Rock Engineering, 1217-1242.

Curden, D., & Varnes, D. (1996). Landslide types and processes. Landslides: Investigation and mitigation, transportation research board special report 247, 36-75.

Fekete, S., & Diedrichs, M. (2013). Integration of Three-dimensional Laser Scanning with Discontinuum Modelling for Stability Analysis of Tunnels in Blocky Rockmasses. International Journal of Rock Mechanics & Mining Sciences, 11-23.

Fu, G., & Ma, G. (2012). Progressive failure analysis and support design of blocky rock mass based on extended key block method. 46th US Rock Mechanics / Geomechanics Symposium. Chicago: ARMA.

Fu, G., Ma, G., Qu, X., & Huang, D. (2016). Stochastic analysis of progressive failure of fractured rock masses containing non-persistent joint sets using key block analysis. Tunnelling and Underground Space Technology, 258-269.

Goodman, R., & Shi, G. (1985). Block Theory and Its Application to Rock Engineering. London: Prentice-Hall.
Grenon, M., & Hadjigeorgiou, J. (2003). Open Stope Stability Using 3D Joint Networks. Rock Mechanics and Rock Engineering, 183-208.

Grenon, M., Landry, A., Hadjigeorgiou, & Lajoie, P. (2017). Discrete Fracture Network Based Drift Stability at the Éléonore Mine. Mining Technology, 22-33.

Hudson, J., & Harrison, J. (2000). Engineering Rock Mechanics. Oxford: Imperial College of Science, Technology and Medicine, University of London, UK.

ITASCA. (2016). 3 Dimensional Discrete Element Code User's Guide. Minneapolis: Itasca Consulting Group.

ITASCA. (2017). Advanced Grid Generation for Engineers and Scientists Griddle and BlockRanger User's Guide. Minneapolis: Itasca Consulting Group Inc.

Jing, L., & Stephansson, O. (2007). Fundamentals of Discrete Element Methods for Rock Engineering Theory and Application. Amsterdam: ELSEVIER.

Lato, M., Diederichs, M., Hutchinson, D., & Harrap, R. (2009). Optimization of LiDAR scanning and processing for automated structural evaluation of discontinuities in rock masses. International Journal of Rock Mechanics and Mining Siences, 1217-1242.

Martin, C., Kaiser, P., & Christiansson, R. (2003). Stress, instability and design of underground excavations. Rock Mechanics and Mining Sciences, 1-21.

Monsalve, J., Baggett, J., Bishop, R., & Ripepi, N. (2018). A Preliminary Investigation for Characterization and Modeling of Structurally Controlled Underground Limestone Mines by Integrating Laser Scanning with Discrete Element Modeling. North American Tunneling Conference. Washington: SME.

Monsalve, J., Baggett, J., Bishop, R., & Ripepi, N. (2019). Application of Laser Scanning for Rock Mass Characterization and Discrete Fracture Network Generation in an Underground Limestone Mine. International Journal of Mining Science and Technology, 131-137.

MSHA. (2016). Metal/Nonmetal Daily Fatality Report. Mine Safety and Health Administration.

NIOSH. (2011). Pillar and Roof Span Design Guidelines for Underground Stone Mines. Pittsburg: National Institute for Occupational Safety and Health.

Pierce, M. (2017). An Introduction to Random Disk Discrete Fracture Network (DFN) for Civil and Mining Engineering Applications. ARMA e-Newslatter 20, 3-8.

Proust, M. (2018). Using JMP. Cary: SAS Institute Inc.

Rogers, S., Bewick, R., Brzovic, A., & Gaudreau, D. (2017). Integrating Photogrametry and Discrete Fracture Network Modelling for Improved Conditional Simulation of Underground Wedge Stability. 8th International Conference in Deep and High Stress Mining, 599-610.